a

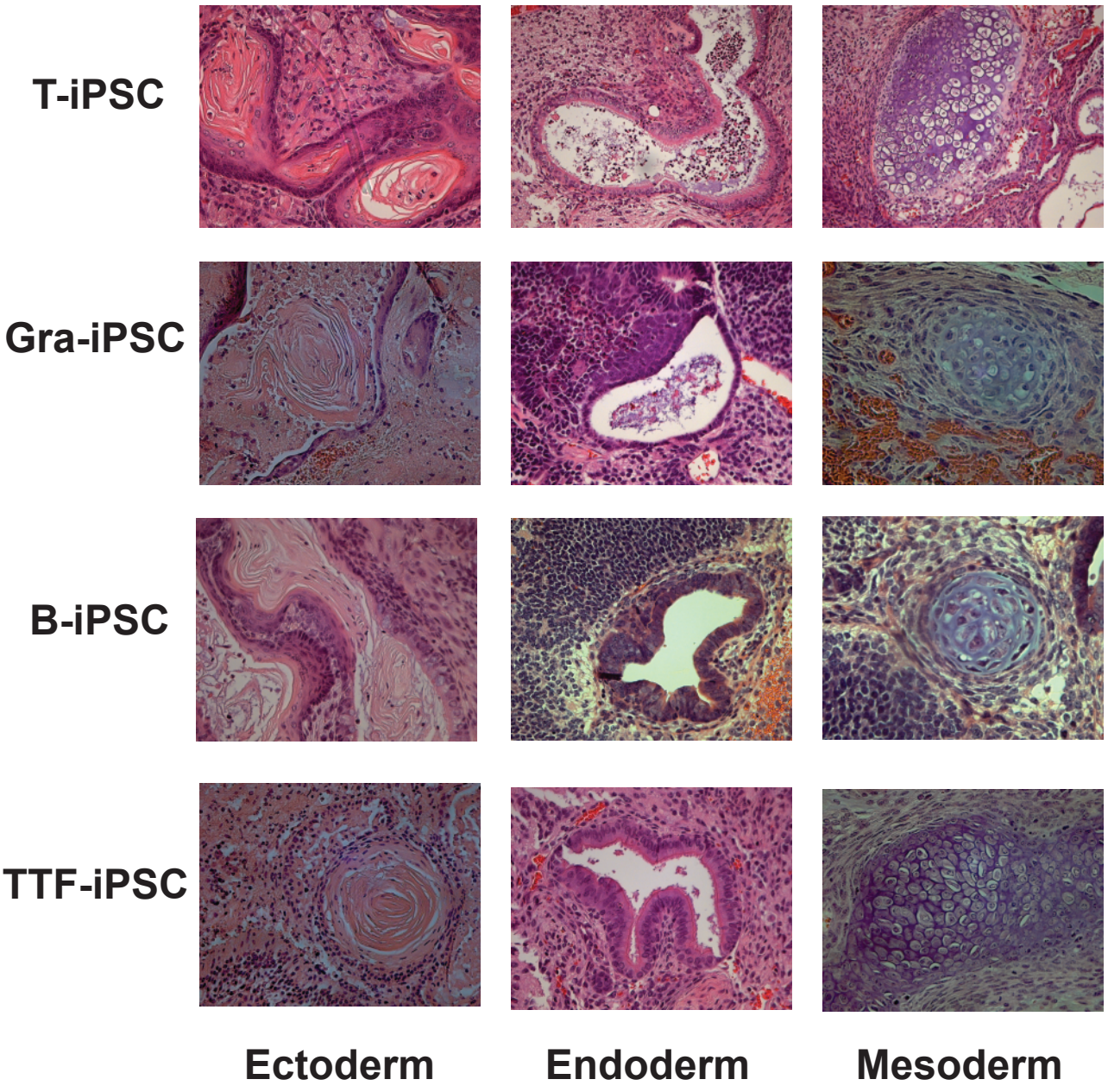

b

Nature Biotechnology: doi: 10.1038/nbt.1667

Supplementary Figure 1

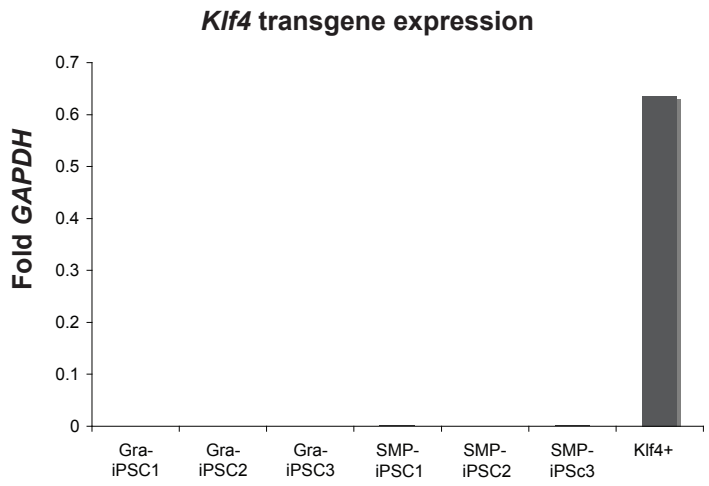

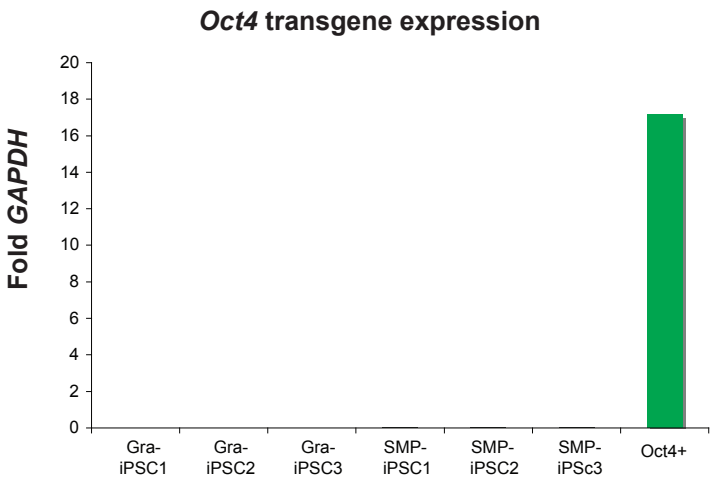

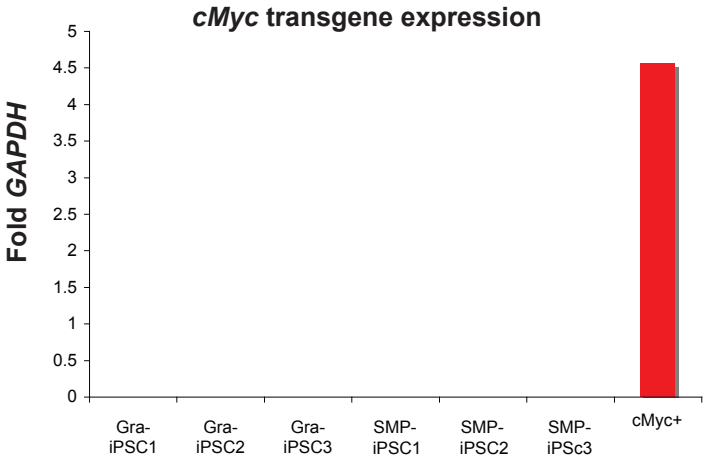

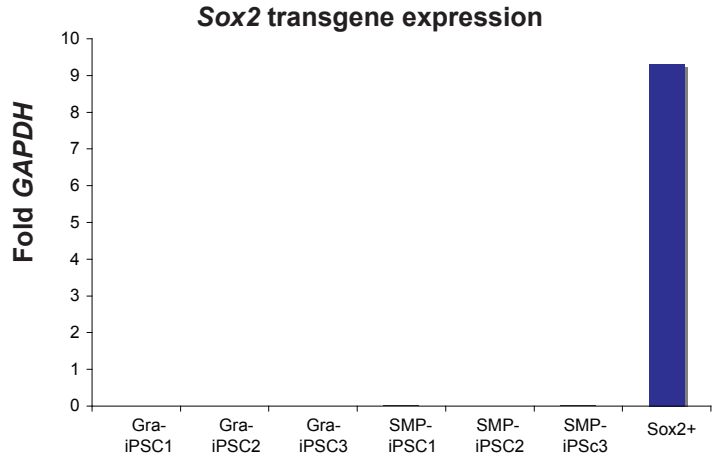

Nature Biotechnology: doi: 10.1038/nbt.1667

Supplementary Figure 2

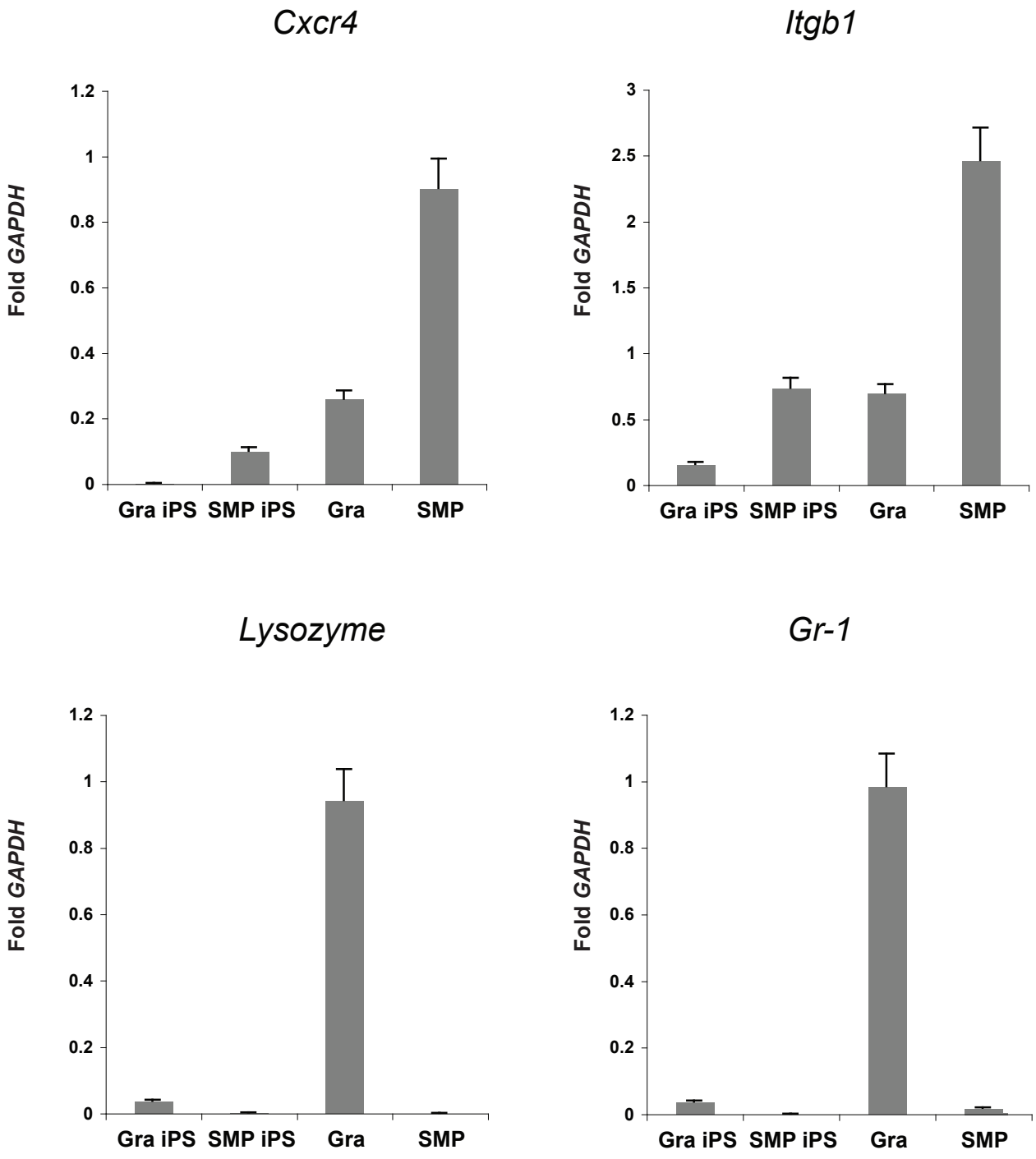

Supplementary Figure 3

Nature Biotechnology: doi: 10.1038/nbt.1667

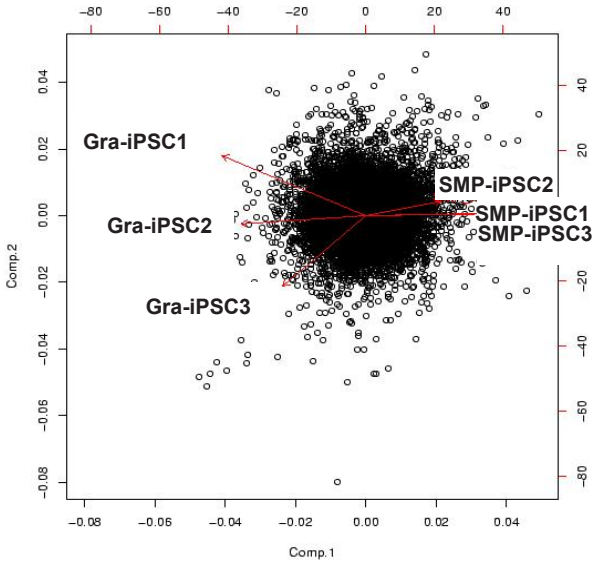

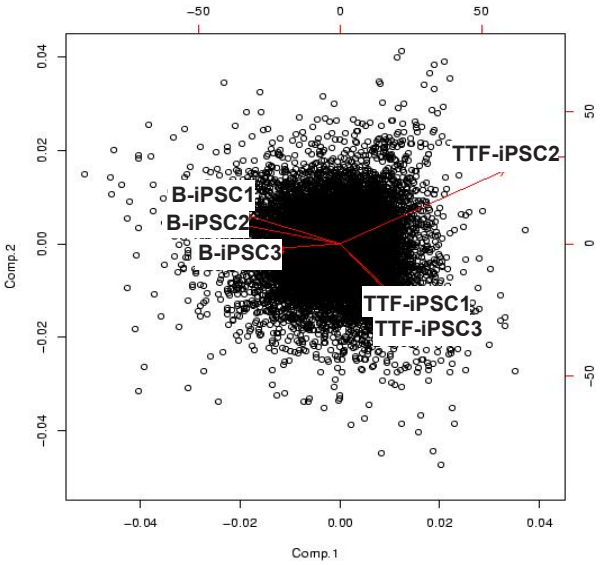

Supplementary Figure 4

Nature Biotechnology: doi: 10.1038/nbt.1667

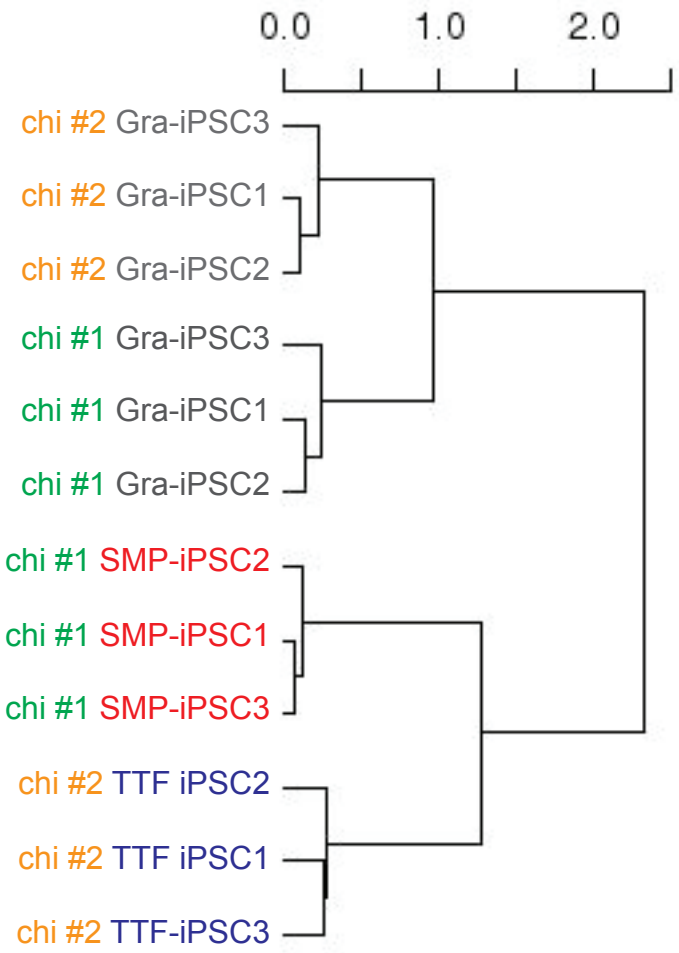

Supplementary Figure 5

Nature Biotechnology: doi: 10.1038/nbt.1667

a

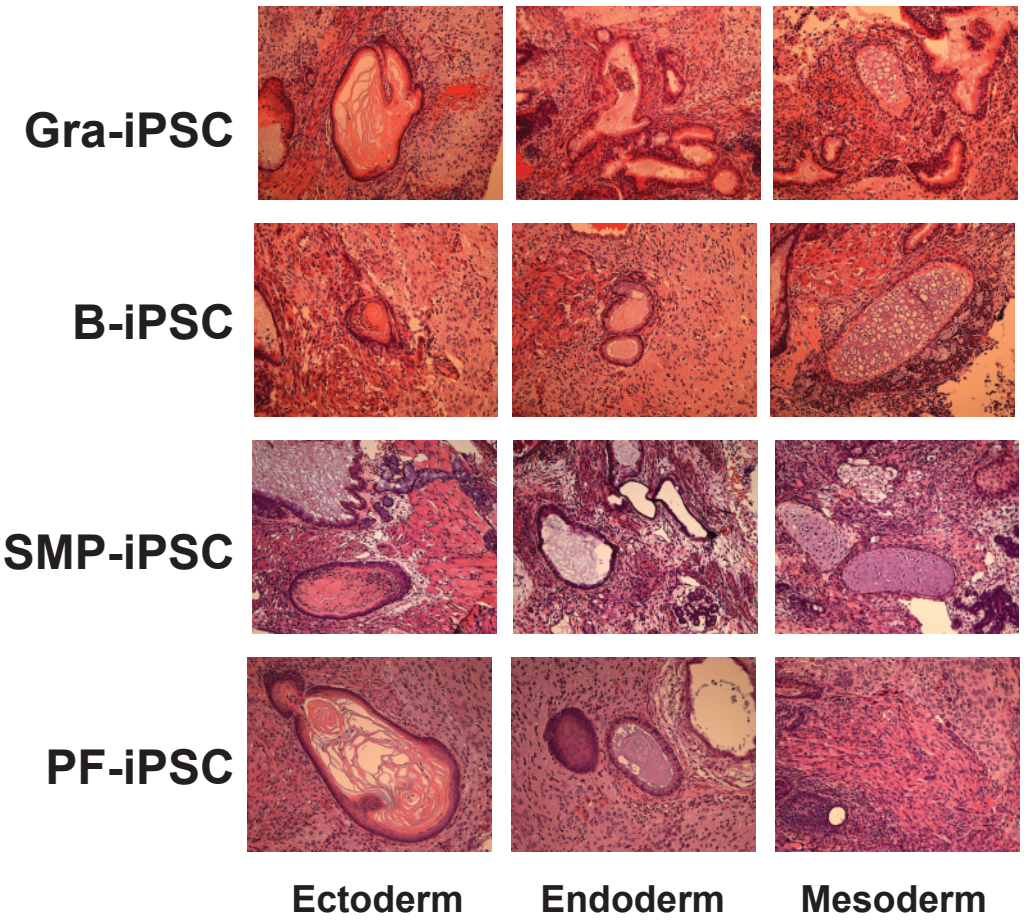

b

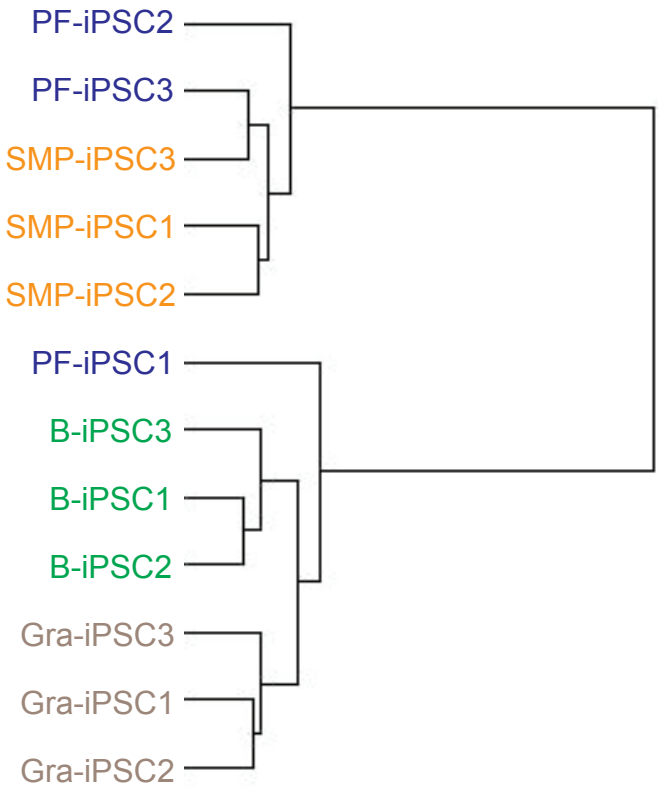

Nature Biotechnology: doi: 10.1038/nbt.1667

Supplementary Figure 6

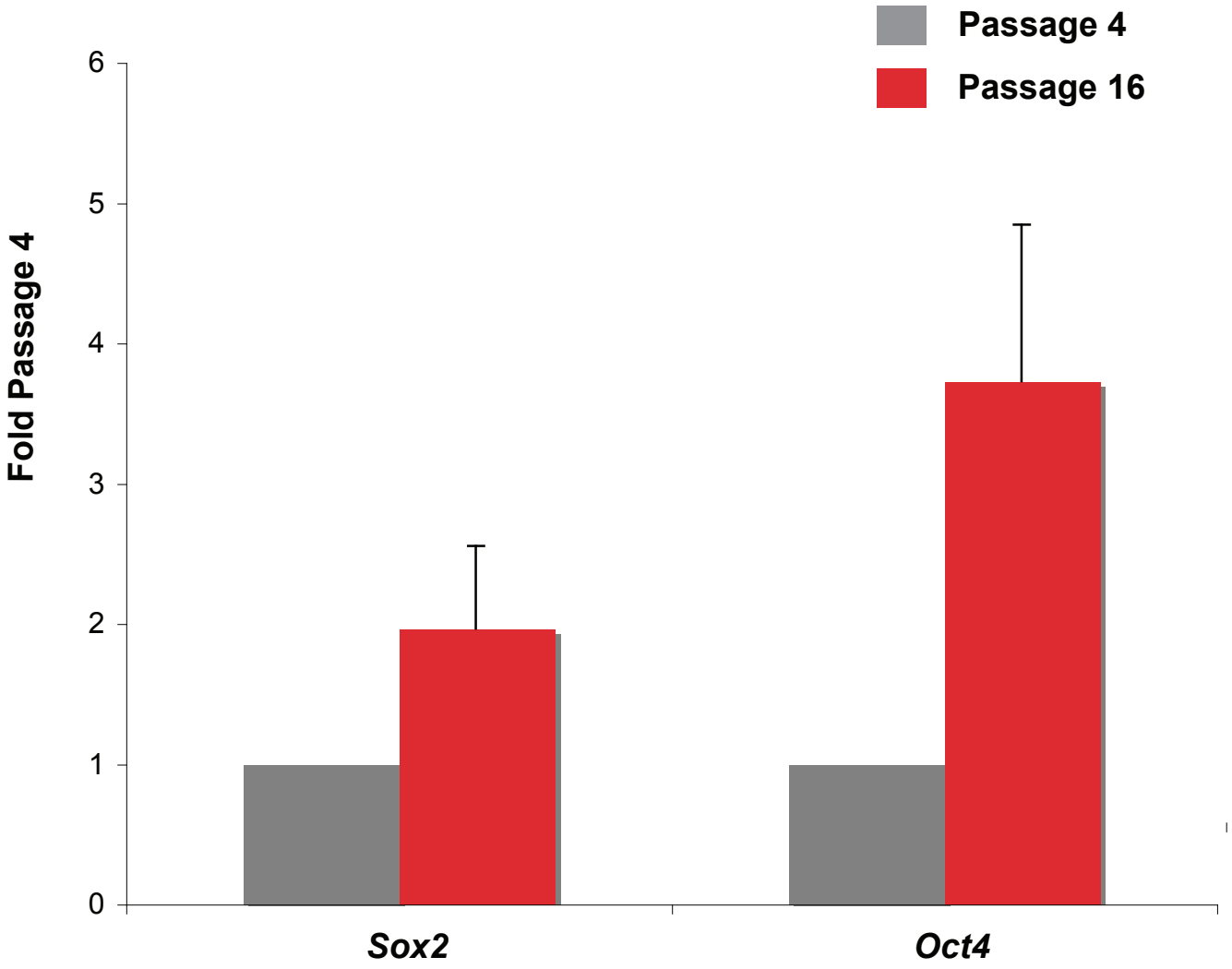

Supplementary Figure 7

Nature Biotechnology: doi: 10.1038/nbt.1667

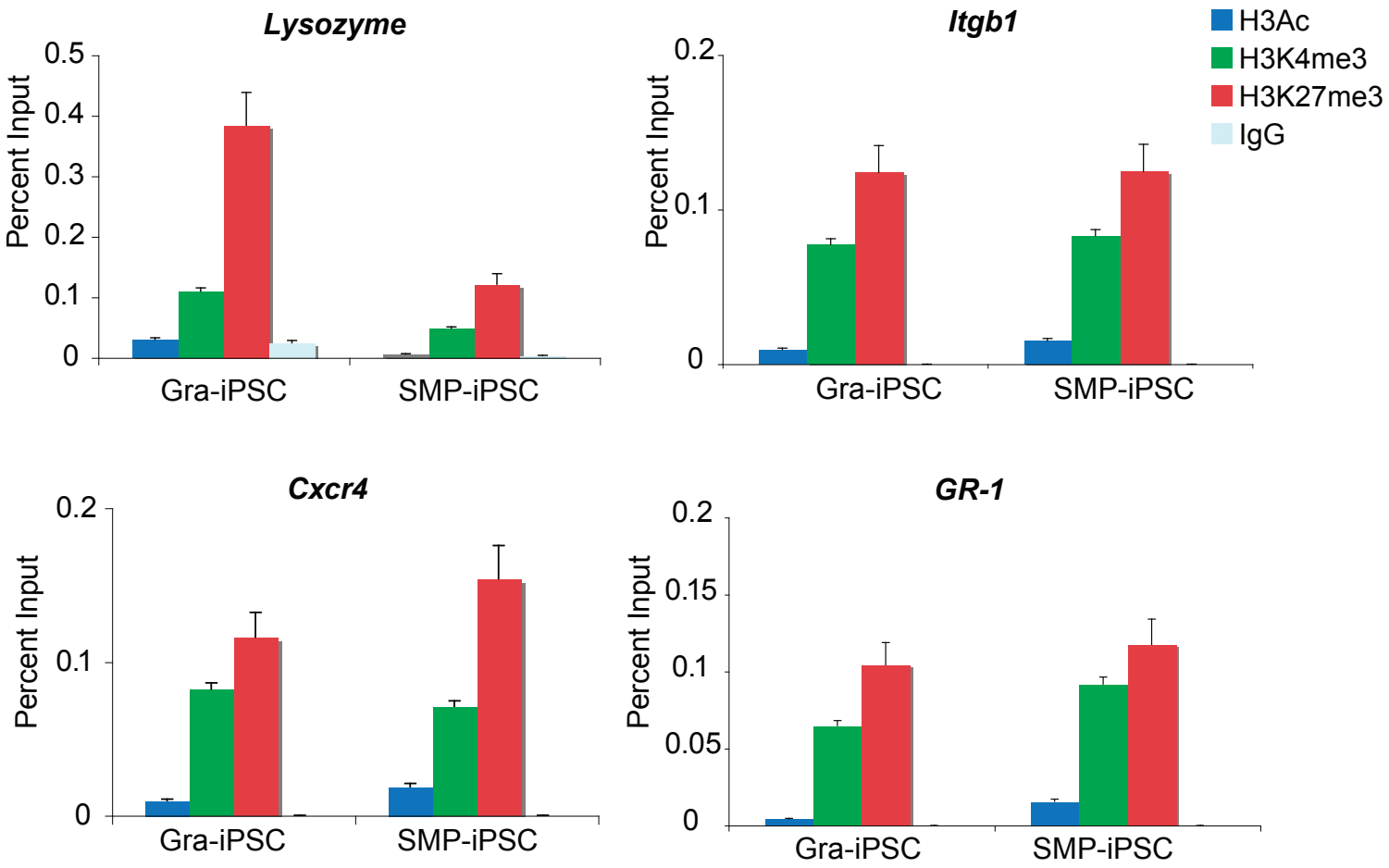

Supplementary Figure 8

Nature Biotechnology: doi: 10.1038/nbt.1667

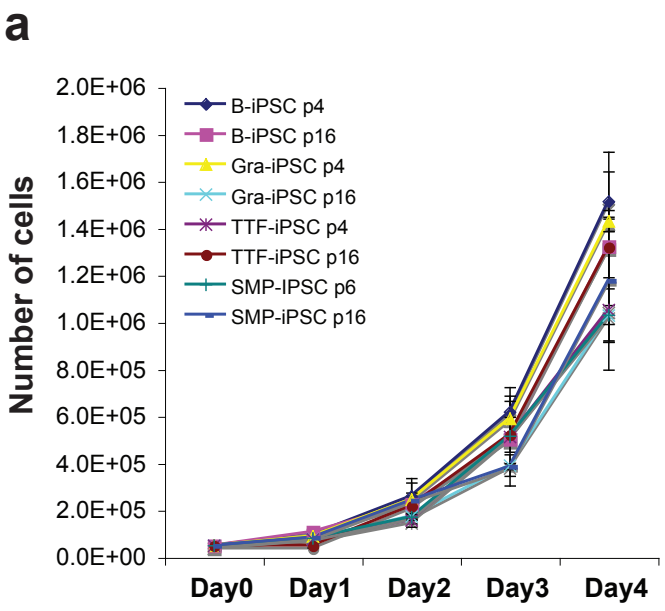

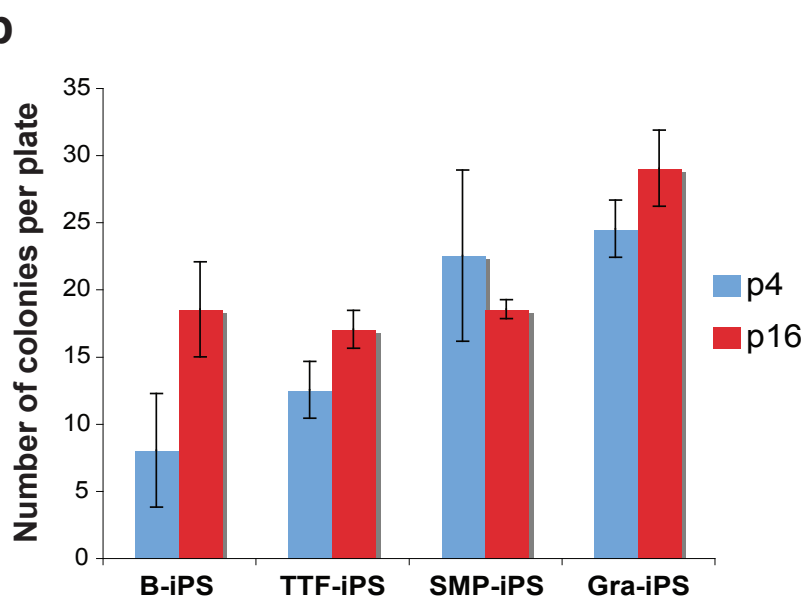

Nature Biotechnology: doi: 10.1038/nbt.1667

Supplementary Figure 9

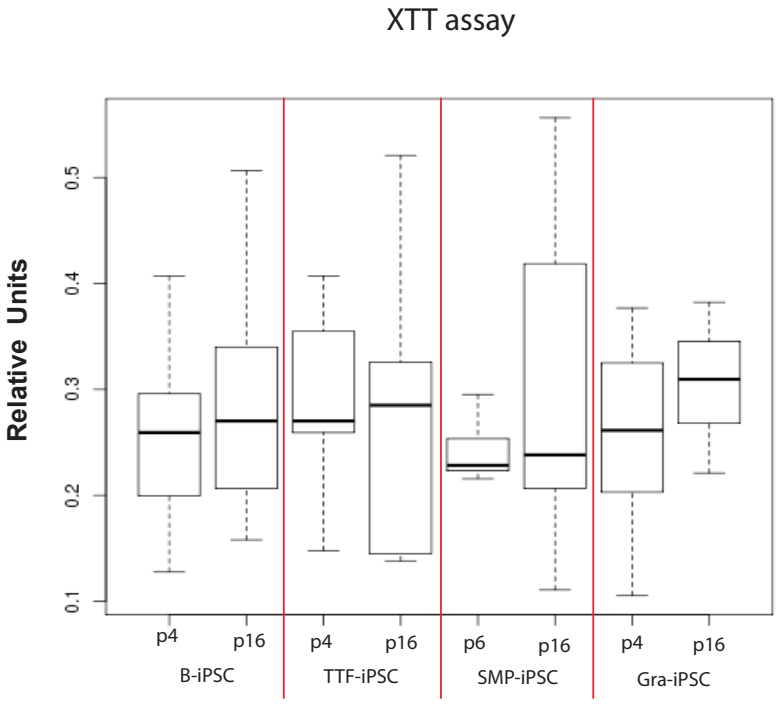

Supplementary Figure 10

Nature Biotechnology: doi: 10.1038/nbt.1667

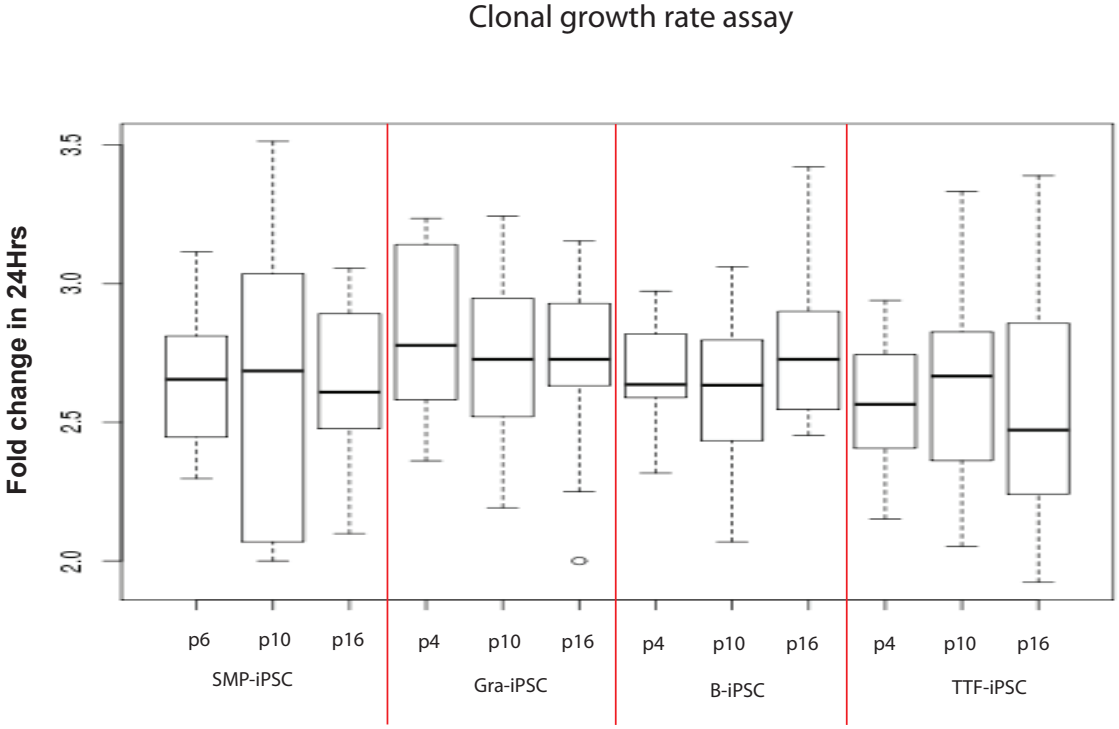

Supplementary Figure 11

Nature Biotechnology: doi: 10.1038/nbt.1667

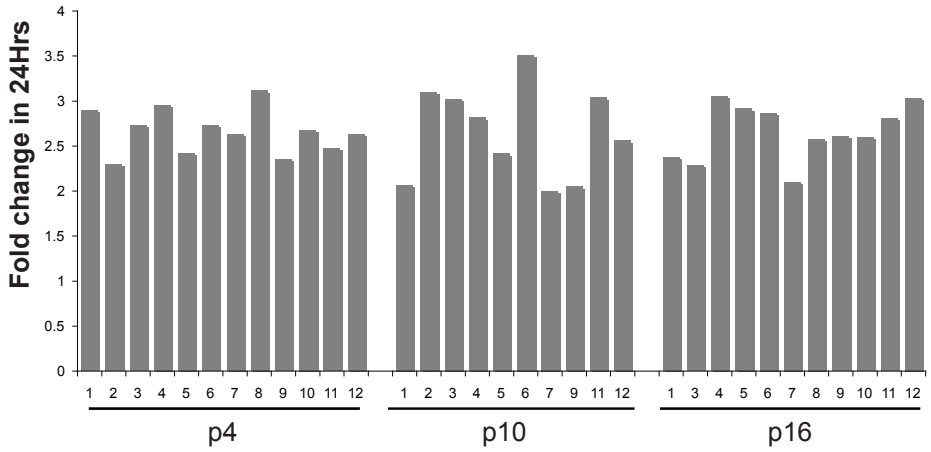

SMP-iPSC

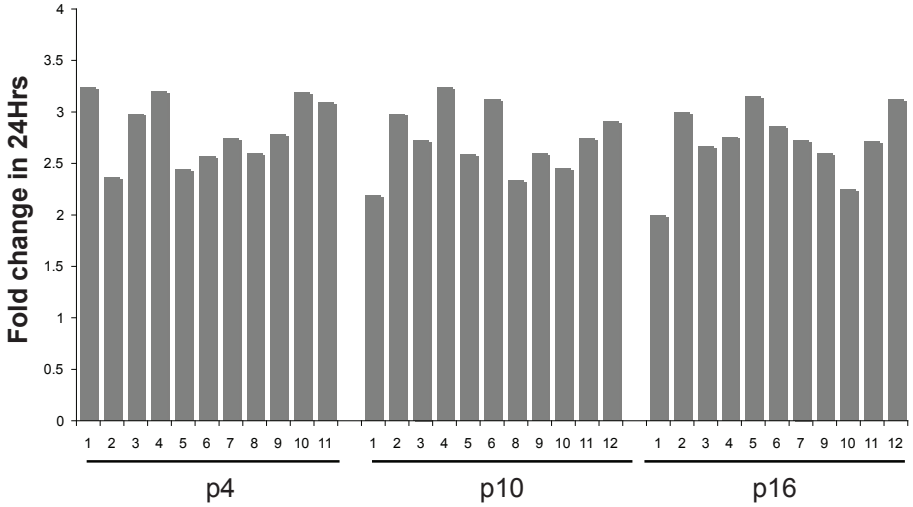

Gra-iPSC

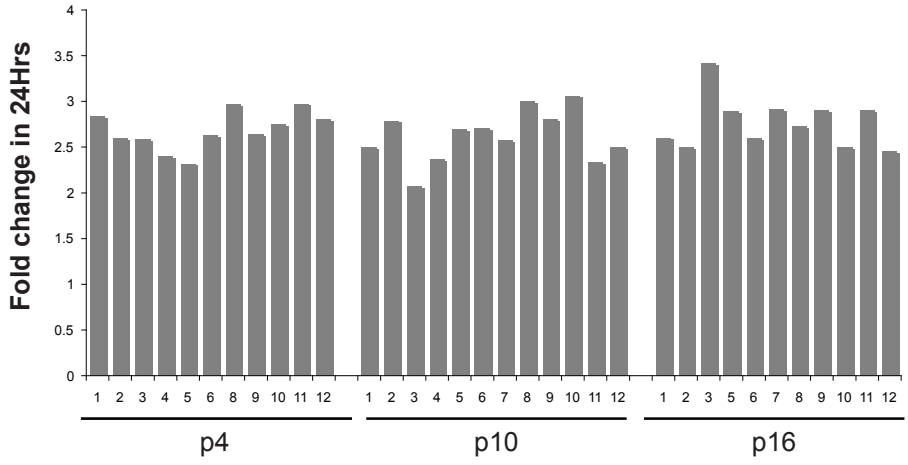

B-iPSC

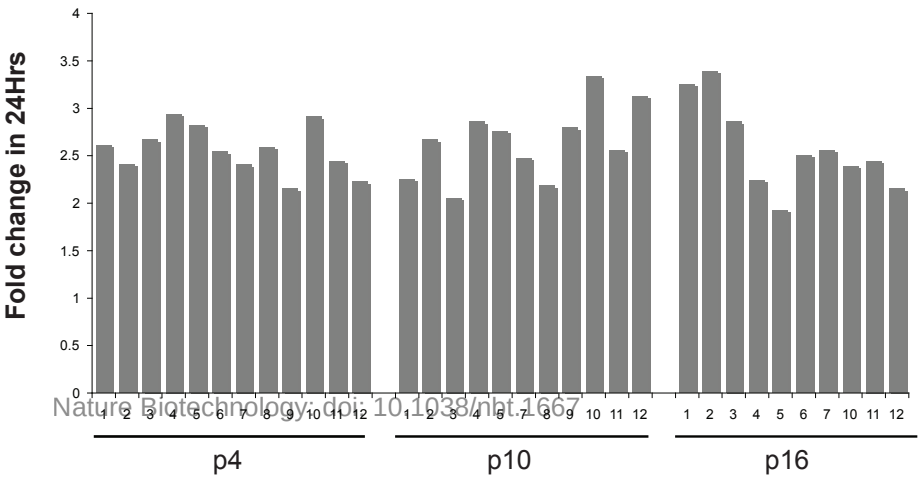

TTF-iPSC

Nature Biotechnology: doi: 10.1038/nbt.1667

Supplementary Figure 12

a

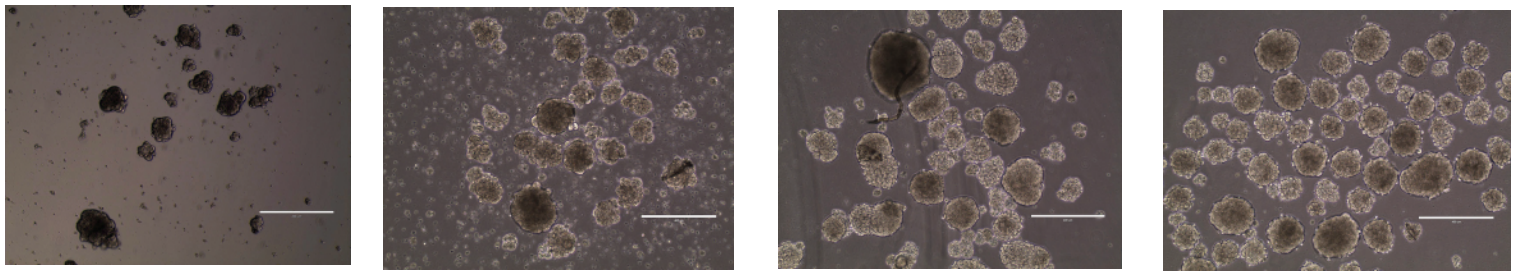

p6 p8 p10 p12

b

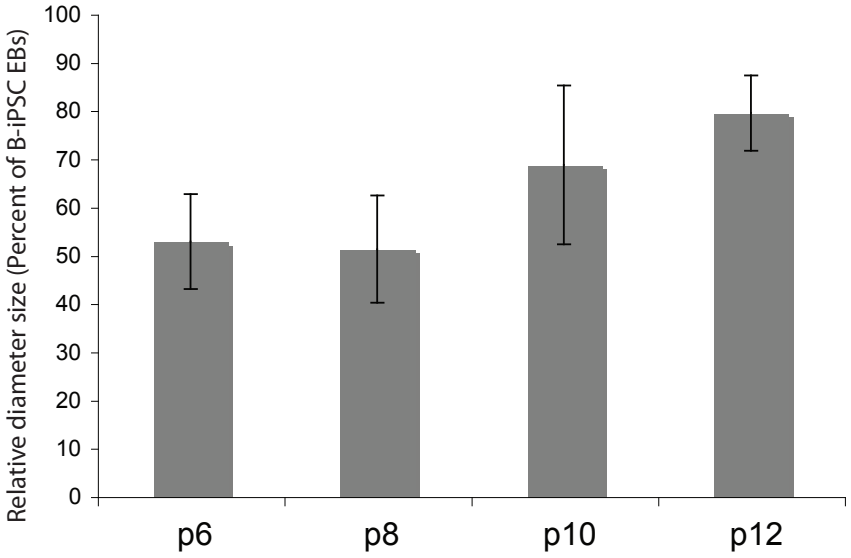

c

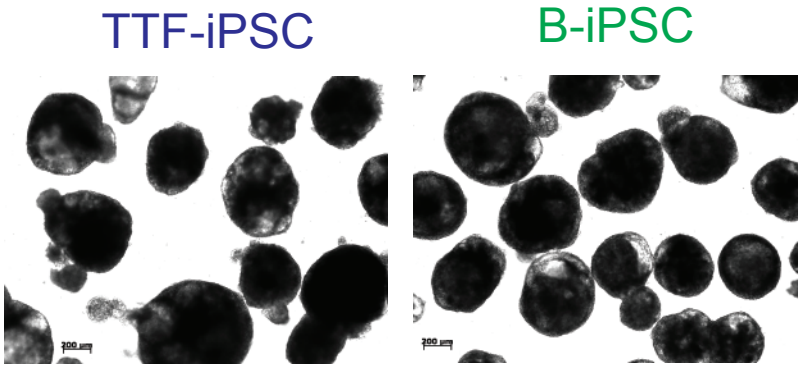

d

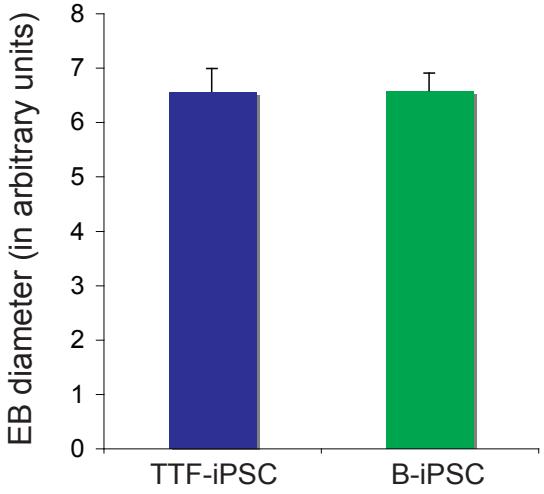

Nature Biotechnology: doi: 10.1038/nbt.1667

Supplementary Figure 13

Supplementary Figure legends

Supplementary Figure 1. Assessment of differentiation potential of representative iPSC lines by teratoma and chimera formation.
(a) Shown are representative H&E stained teratoma sections produced from the indicated iPSC lines, demonstrating differentiation into derivatives of the three germlayers. (b) Representative coat color chimera obtained by blastocyst injection of SMP-iPSCs.

Supplementary Figure 2. Efficient silencing of viral transgenes in iPSCs.
Quantification of the expression levels of Klf4 (upper left panel), Oct4 (upper right panel), cMyc (lower left panel) and Sox2 (lower right panel) by quantitative PCR in iPSCs derived from SMPs (SMP-iPSCs) and granulocytes (Gra-iPSCs) following doxycycline withdrawal. Positive control for the expression of the transgenes are included; Klf4 (black bar), Oct4 (green bar), cMyc (red bar) and Sox2 (blue bar). The values were normalized to GAPDH expression (n=3).

Supplementary Figure 3. Cell type-specific marker expression.
Quantification of the expression levels of somatic-specific candidate genes for SMPs, *Cxcr4* and *Integrin B1 (Itgb1)*, and for granulocytes, *lysozyme* and *Gr-1,* by quantitative PCR. The levels of these transcripts related to GAPDH are shown in Granulocytes (gray bars) and SMPs (red bars). The error bars depict the S.E.M. (n=3)

Supplementary Figure 4. Principal component analysis of iPSCs.
Graphical representation of principal component analysis based on expression profiles of SMP-iPSCs and Gra-iPSCs (left panel) from chimera #1, TTF-iPSCs and B-iPSCs (right panel) from chimera #2. Note that iPSCs cluster based on their cell of origin.

Supplementary Figure 5. Effects of iPSCs derived from different animals on gene expression.

Hierarchical unsupervised clustering based on the expression profiles of SMP-iPSCs and Gra-iPSCs from chimera #1 and Gra-iPSCs and TTF-iPSCs from chimera #2 using the correlation distance and the Ward method. Note that **i**PSCs cells cluster first based on their cell of origin and second by the animal from which they were derived.

Supplementary Figure 6. Differentiation potential and gene expression analysis of iPSCs derived from "reprogrammable mice".

(a) Shown are representative H&E stained teratoma sections produced from the indicated iPSC lines, demonstrating differentiation into derivatives of the three germlayers. (b) Unsupervised hierarchical clustering of gene expression data of iPSC clones derived from indicated somatic cells at p4. Note clustering of samples into groups depending on cell of origin. The failure of one PF-iPSC sample to cluster within its group may be explained by the heteropgeneity of the starting population.

Supplementary Figure 7. Effect of passaging on pluripotency gene expression.

Quantification of the expression levels of Sox2 and Oct4 in iPSCs harvested at passage 4 (grey bars) and passage 16 (red bars) by quantitative PCR. The values were normalized by GAPDH expression and expressed as fold over passage 4, the error bars depict the S.E.M. (n=6).

Supplementary Figure 8. Histone modifications in iPSCs at passage 16.

Chromatin inmunoprecipitation (ChIP) for H3 pan-acetylated (H3Ac, in blue), H3K4 trimethylated (K4(CH3)3, in green), H3K27 trimethylated (K27(CH3)3, in red) and isotype control (IgG, in light blue) of Granulocytes (Gra), SMPs, Gra-iPSCs and SMP-iPSCs at passage 16. The promoters of the indicated genes were analyzed. The error bars depict the S.E.M. (n=3)

Supplementary Figure 9. Growth rates of bulk iPSC cultures derived from different cells of origin.

(a) Growth curve of iPSCs from different cells of origin at passage 4 (p4) and p16. The graph depicts total number of cells on four consecutive days. **(b)** Single cell cloning potential of different iPSCs lines at p4 (blue bars) and p16 (red bars). Shown is the fraction of cells giving rise to discernible iPSC colonies. The error bars depict the S.E.M. (n=2)

Supplementary Figure 10. Relative growth of single iPSCs clones.

Boxplot representing the XTT signal of single iPSC clones derived from different cell types at passage 4 (p4) and p16 after 7 days in culture (n=20). Cell growth was measured by a colorimetric assay that detects metabolic activity of cells.

Supplementary Figure 11. Growth rate of single cloned iPSCs from different cells of origin (boxplot representation).

Boxplot representing the increase in cell numbers of clonal iPSC lines within 24 hour window. Depicted are iPSCs from differentent cells of oringin at passage 4 (p4), p10 and p16 (n=12).

Supplementary Figure 12. Growth rate of single cloned iPSCs from different cell of origin (bargraph representation).

Bars representing the increase in cell numbers of clonal iPSC lines within 24 hour window. Depicted are iPSCs from differentent cells of oringin at passage 4 (p4), p10 and p16. Same data as in Suppl. Figure 9.

Supplementary Figure 13. Effect of passaging of iPSCs on EB size.

(a) Images showing EBs derived from TTF-iPSCs at passage (p) 6,8,9,10,11 and 12. **(b)** Quantification of EB size derived from TTF-iPSCs relative to B-iPSCs. The error bars depict the S.D. (average n=100)**. (c)** Images showing EBs derived from B-iPSCs and TTF-iPSCs at passage 16. **(d)** Quantification of EB size

derived from TTF-iPSCs (blue bar) and B-iPSCs (green bar) shown in (c); the diameter of EBs was measured using arbitrary units (AU). The error bars depict the S.E.M. (n=25)

Nature Biotechnology: doi: 10.1038/nbt.1667

Supplementary Table 1

Molecular and functional characterization of iPSCs.

Chimera	iPSC line	Endog. Sox2	Endog. Oct4	Endog. Nanog	Oct4 promoter demethylation	Teratoma	Chimera
1	Gra-iPSC1	1.029	0.839	1.023	Yes	Yes	Yes
1	Gra-iPSC2	1.045	0.749	1.126	Yes	Yes	N/D
1	Gra-iPSC3	1.151	0.741	1.213	Yes	Yes	N/D
1	SMP-iPSC1	1.014	0.734	0.963	Yes	Yes	N/D
1	SMP-iPSC2	1.118	0.745	0.975	Yes	Yes	Yes
1	SMP-iPSC3	1.037	0.668	0.900	Yes	Yes	Yes
2	B-iPSC1	1.109	0.818	1.121	Yes	Yes	N/D
2	B-iPSC2	1.029	0.800	1.192	Yes	Yes	N/D
2	B-iPSC3	0.975	0.715	1.277	Yes	Yes	N/D
2	TTF-iPSC1	1.048	0.541	1.013	Yes	Yes	Yes
2	TTF-iPSC2	0.816	0.455	1.208	Yes	Yes	N/D
2	TTF-iPSC3	0.824	0.592	1.183	Yes	Yes	N/D
2	Gra-iPSC1	0.996	0.710	1.177	Yes	Yes	Yes
2	Gra-iPSC2	1.044	0.649	1.240	Yes	Yes	N/D
2	Gra-iPSC3	0.872	0.626	1.003	Yes	Yes	N/D
2	T-iPSC1	0.980	0.690	0.948	Yes	Yes	Yes
2	T-iPSC2	0.732	0.712	0.843	Yes	Yes	Yes
2	T-iPSC3	1.003	0.620	0.602	Yes	Yes	N/D

N/D - Not determined ; indicated values were taken from expression arrays and shown relative to ESC values (set at 1.0)
Oct4 promoter demethylation status was taken from HELP data.